Journal Pre-proof

Effective hopping between magnetic impurities in silicene

J. Villarreal, J. Juan, P. Jasen, J.S. Ardenghi

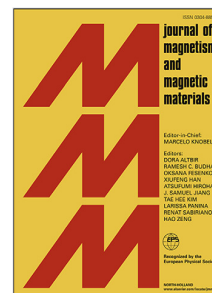Please cite this article as: J. Villarreal, J. Juan, P. Jasen et al., Effective hopping between magnetic impurities in silicene, *Journal of Magnetism and Magnetic Materials* (2022), doi: https://doi.org/10.1016/j.jmmm.2022.169726.

This is a PDF file of an article that has undergone enhancements after acceptance, such as the addition of a cover page and metadata, and formatting for readability, but it is not yet the definitive version of record. This version will undergo additional copyediting, typesetting and review before it is published in its final form, but we are providing this version to give early visibility of the article. Please note that, during the production process, errors may be discovered which could affect the content, and all legal disclaimers that apply to the journal pertain.

Effective hopping between magnetic impurities in silicene

J. Villarreal[†], J. Juan[†], P. Jasen[†] and J. S. Ardenghi[†*]

[†]IFISUR, Departamento de Física (UNS-CONICET)

Avenida Alem 1253, Bahía Blanca, Buenos Aires, Argentina

July 15, 2022

Abstract

In this work we analyze the effects of the conduction electrons on the hopping function between two magnetic impurities located in the A sublattice in silicene placed in an external electric field. By using the Schrieffer-Wolff transformation we analyze the dependence of the effective hopping on the distance between the magnetic adatoms. By using particle number conservation, the spectrum for different occupation numbers is studied for different values of the Hubbard parameter, the electric field and the inter-impurity distance. We show that for half-filling an ionic to covalent ground state transition and viceversa can be achieved for a specific electric field strength. Finally, we explore the partition function and we study the average energy and average occupation as a function of temperature, obtaining a pattern of Mott plateaus.

1   Introduction

Among 2D materials, silicene has many interesting properties as graphene and is a subject of experimental and theoretical research due to its compatibility with the current Si-based electronic technology ([1], [2], [3], [4], [5], [6], and [7]). First-principles calculations have shown that the buckled-structure of isolated silicene is more stable than the corresponding planar geometry of this material [8] and the two interpenetrating sublattices displaced vertically due to the tetrahedral sp_3 hybridization, opens an electrically tunable band dispersion [9]. In turn, the large spin-orbit interaction allows the quantum spin Hall effect to be experimentally accessible [10], which implies that silicene is very sensitive to external electric and magnetic fields and shows remarkable subtleties in the De Haas-Van Alphen effect ([11], [12] and [13]). Nowadays, quantum computing requires the realization of quantum bits, which can be implemented via quantum impurity systems ([14], [15], [16]) such as magnetic adatoms and molecules on surfaces or nano-structured gate-controlled devices that allow to combine usual electronics with spintronics ([17], [18], [19] and [20]). On silicene, impurity atoms can be deposited at different sites, where the most usual ones are the six-fold hollow site of the honeycomb lattice, on top of a silicon atom and the two-fold bridge site of neighboring silicon atoms [21]. The presence of a magnetic adatom in a metal has been successfully studied using the Anderson model ([22], [23]), which has recently also been applied to studying magnetic moment formation in graphene and silicene ([24], [25]) and where it has been shown that the coupling of an adatom to a 2D material results in a much easier formation of magnetic moment due to the anomalous broadening of the electronic levels of the adatoms [26].

When two magnetic impurities are present little is known about the effect of the inter-impurity interaction on the localized moments. Ab initio calculations show that the interaction between impurities may lead to a subtle consequence in the formation of a local magnetic moment in 2D materials [27]. Considering a constant electron hopping between impurities, it has been found that the interaction between two impurities brings about a significant modification in the impurity self-energy, which pushes

*email: jsardenghi@gmail.com, fax number: +54-291-4595142

the impurity energy across the zero energy point, thus leading to the splitting of the impurity magnetization boundary into three peaks. Given a fixed energy of some impurity, the magnetic region exhibits an asymmetric behavior between the cases of positive and negative energy of the other impurity. Additionally the inter-impurity interaction tends to suppress the local magnetic moment on impurities ([28], [29]). By controlling the interaction between impurities via the adjustment of the chemical potential, a weak repulsion has been observed when the two atoms reside on the same sublattice, while an attraction of stronger intensity is noticed when they are on different sublattices [30]. It must be stressed that considering a constant electron hopping between magnetic impurities is reasonable for specific fixed positions but this assumption is only applicable for a fixed number of electrons. Motivated by the lack of literature about the interplay of the effective tunneling between the magnetic impurities with different occupation numbers, we present an analytical study of the distance-dependent hopping function between the two impurities in silicene with spin-orbit coupling and external electric field, which allows us to map the emerging scattering terms onto an effective tunneling between the impurities. By applying the Schrieffer-Wolff transformation (SW), and solving a coupled equations for the coefficients of the S matrix, we obtain the tunnelling between impurities for different occupancy numbers. We also discuss the spectrum of the two-site Hubbard model with effective hopping between magnetic sites near the Dirac point and for arbitrary distances between the magnetic adatoms. Furthermore, we analyze the average number occupation for different temperatures where Mott plateaus are shown for specific ranges of impurity distances. This work will be organized as follows: In section II, the two impurity Anderson model (TIAM) in silicene is described and the SW transformation is applied. In section III, the results are shown for different occupation numbers and a discussion is given. The principal findings of this paper are highlighted in the conclusion.

2 Theoretical model

Our starting point is the tight binding Hamiltonian of the total system

$$H = H_{sil} + H_U + H_{hyb} \tag{1}$$

where

$$H_{sil} = -t \sum_{\langle i,j \rangle, \sigma} a_{i,\sigma}^{\dagger} b_{j,\sigma} + h.c + \frac{i\lambda}{3\sqrt{3}} \sum_{\langle\langle i,j \rangle\rangle, s} s(\nu_{ij} a_{i,s}^{\dagger} a_{j,s} + \nu_{ij} b_{i,s}^{\dagger} b_{j,s}) \tag{2}$$
$$+ V_z \sum_{i,s} (a_{i,s}^{\dagger} a_{i,s} - b_{i,s}^{\dagger} b_{i,s})$$

The first contribution to H_{sil} is the kinetic energy of electrons in silicene, the second term represents the effective spin-orbit coupling with $\lambda = 3.9$ meV for silicene (see [31]) and $\nu_{ij} = (\mathbf{d}_i \times \mathbf{d}_j)/|\mathbf{d}_i \times \mathbf{d}_j| = \pm 1$, depending on the orientation of the two nearest neighbor bonds $\mathbf{d}_i$ and $\mathbf{d}_j$ that connect the next nearest neighbors $\mathbf{d}_{ij}$ (see [32] and [33]) and the third term represents the application of an external electric field perpendicular to the silicene layer, where $V_z = lE_z$ is the electric potential and $l = 0.44$Å is the distance of each sublattice with respect to the middle of the buckling in silicene. $a_{i,\sigma}^{\dagger}(a_{i,\sigma})$ are the creation (annihilation) operators acting in the sublattice A and $b_{i,\sigma}^{\dagger}(b_{j,\sigma})$ are the creation (annihilation) operators with spin $\sigma = \pm 1$ in the site i of the A and B sublattices respectively and $\langle i,j \rangle$ indicates sum over nearest neighbors and $t = 1.6$eV. The second contribution to H comes from the Anderson model describing two identical magnetic impurities with a single orbital of energy ϵ_0 and Coulomb repulsion U, $H_U = \epsilon_0 \sum_{J,\sigma} n_{J\sigma} + U \sum_J n_{J\uparrow} n_{J\downarrow}$, where $n_{J\sigma} = f_{J\sigma}^{\dagger} f_{J\sigma}$ is the occupation number of the magnetic impurity and $f_{J,\sigma}^{\dagger}(f_{J,\sigma})$ are the creation (annihilation) operators acting on the impurity sites $J = 1, 2$ located in sublattice A of silicene. The third contribution to H is the hybridization Hamiltonian of the magnetic impurities with the host lattice $H_{hyb} = V \sum_{J=1,2;\sigma} (a_{J,\sigma}^{\dagger} f_{J\sigma} + f_{J\sigma}^{\dagger} a_{J,\sigma})$, where $\mathbf{R}_J$ are
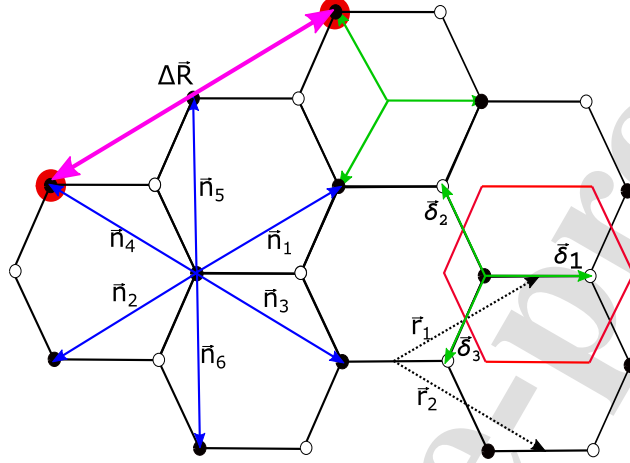
Figure 1: Geometry of silicene with two magnetic impurities (red dots) placed on the A sublattice.

the fixed positions of the two magnetic impurities. In figure 1, a top view schematic picture of the silicene honeycomb lattice can be seen, where the two magnetic impurities are located in sublattice A. Considering the Fourier transform of the creation and annihilation operators $a_{j,s} = \frac{1}{\sqrt{N}}\sum_{\mathbf{k}} e^{-i\mathbf{kR}_j} a_{\mathbf{k},\sigma}$

and $b_{j,s} = \frac{1}{\sqrt{N}}\sum_{\mathbf{k}} e^{-i\mathbf{kR}_j} b_{\mathbf{k},\sigma}$ where N is the number of primitive cells, the Hamiltonian H becomes

$$H = \sum_{\mathbf{k},\sigma} \phi_{\mathbf{k}} a^{\dagger}_{\mathbf{k},\sigma} b_{\mathbf{k},\sigma} + h.c. + \sum_{\mathbf{k},\sigma} \frac{i\xi_{\mathbf{k}}}{3\sqrt{3}} \Delta_{\sigma}(a^{\dagger}_{\mathbf{k},\sigma} a_{\mathbf{k},\sigma} - b^{\dagger}_{\mathbf{k},\sigma} b_{\mathbf{k},\sigma}) \tag{3}$$

$$+ H_U + \sum_{J,\mathbf{k},\sigma}(V_{J\mathbf{k}} a^{\dagger}_{\mathbf{k},\sigma} f_{j\sigma} + V^{*}_{J\mathbf{k}} f^{\dagger}_{j\sigma} a_{\mathbf{k},\sigma})$$

where $\phi_{\mathbf{k}} = -t\sum_{i=1}^{3} e^{i\mathbf{k}\cdot\delta_{\mathbf{i}}}$ and $\xi_{\mathbf{k}} = \sum_{i=1}^{6} e^{i\mathbf{k}\cdot\mathbf{n_i}}$, where $\delta_{\mathbf{1}} = \frac{a}{2}(1,\sqrt{3},0)$, $\delta_2 = \frac{a}{2}(1,-\sqrt{3},0)$ and $\delta_3 = a(1,0,0)$ are the next nearest neighbor vectors, whereas $\mathbf{n_1} = -\mathbf{n_2} = \mathbf{a_1}$, $\mathbf{n_3} = -\mathbf{n_4} = \mathbf{a_2}$ and $\mathbf{n_5} = -\mathbf{n_6} = \mathbf{a_1} - \mathbf{a_2}$ are the six next-nearest neighbor hopping sites (see figure 1) that connect identical sublattice sites. In the long wavelength approximation, $\phi_{\mathbf{k}} = \epsilon_k e^{i\eta}$ and $\xi_{\mathbf{k}} = -i3\sqrt{3}$, where $\epsilon_k = \hbar v_F k$, $k = |\mathbf{k}| = \sqrt{k_x^2 + k_y^2}$ and $\eta = \arctan(\frac{k_y}{k_x})$. The coefficient $V_{J\mathbf{k}} = \frac{V e^{i\mathbf{k}\cdot\mathbf{R}_J}}{\sqrt{N}}$ contains the dependence with the magnetic impurity position. It is worth mentioning that, since the two inequivalent valleys in the monolayer silicene are separated in the Brillouin zone by a large momentum gap, the intervalley scattering is neglected ([34], [35] and [36]) and only one valley will be considered. The factor $\Delta_{\sigma} = \sigma\lambda - V_z$ contains the spin-orbit coupling and the application of an external electric field E_z through the electric potential V_z. We can diagonalize H_{sil} by introducing the valence/conduction operators

$$c^{(s)}_{\mathbf{k}\sigma} = \chi^{(s)}_{k\sigma}(a_{\mathbf{k},\sigma} + se^{-i\phi_{\mathbf{k}}}\xi^{(s)}_{k\sigma} b_{\mathbf{k},\sigma}) \tag{4}$$

where $\chi^{(s)}_{k\sigma} = \sqrt{\frac{\epsilon_{k\sigma} + s\Delta_{\sigma}}{2\epsilon_{k\sigma}}}$ and $\xi^{(s)}_{k\sigma} = \frac{1}{\epsilon_k}(\epsilon_{k\sigma} - s\Delta_{\sigma})$, and where $s = +1(-1)$ for the conduction (valence) band. The eigenvalues of H_{sil} are $\epsilon_{k\sigma s} = s\epsilon_{k\sigma}$ where $\epsilon_{k\sigma} = \sqrt{\epsilon_k^2 + \Delta_{\sigma}^2}$. When we consider the two valleys, Δ_{σ} depends on the valley index as $\Delta_{\sigma}^{\eta} = \eta\sigma\lambda - V_z$ (see [31]). Is not difficult to show that $\{c^{(s)}_{\mathbf{k}\sigma}, c^{(s')\dagger}_{\mathbf{k}'\sigma'}\} = \delta_{\mathbf{kk}'}\delta_{\sigma\sigma'}\delta_{ss'}I$, where I is the identity operator and the Hamiltonian H in the new basis

3

reads

$$H = \sum_{\mathbf{k},\sigma,s} s\epsilon_{k\sigma}c^{(s)\dagger}_{\mathbf{k},\sigma}c^{(s)}_{\mathbf{k},\sigma} + \sum_{J,\mathbf{k},\sigma,s}(\overline{V}^{(s)}_{J\mathbf{k}\sigma}c^{(s)\dagger}_{\mathbf{k}\sigma}f_{J\sigma} + \overline{V}^{(s)*}_{J\mathbf{k}\sigma}c^{(s)}_{\mathbf{k}\sigma}f^{\dagger}_{J\sigma}) + H_U \tag{5}$$

where $\overline{V}^{(s)}_{J\mathbf{k}\sigma} = \chi^{(s)}_{k\sigma}V_{J\mathbf{k}}$. In order to obtain the effective interaction between the magnetic impurities sorrounded by random impurities, we can apply the Schrieffer–Wolff transformation ([37], [38], [39]). By writing $H = H_0 + H_{hyb}$ and considering $H_0 = H_{sil} + H_U$ as the free Hamiltonian and H_{hyb} the interaction, a unitary anti-Hermitian operator S can be obtained such that the unitary transformation $e^S H e^{-S}$ of H reads

$$H' = e^S H e^{-S} = H_0 + \frac{1}{2}[S, H_{hyb}] + O(S^2) \tag{6}$$

The S operator is obtained in Appendix and reads

$$S = \sum_{J,\mathbf{k},\sigma,s}(A^{(s)}_{J\mathbf{k}\sigma} + B^{(s)}_{J\mathbf{k}\sigma}n_{J-\sigma})c^{(s)\dagger}_{\mathbf{k}\sigma}f_{J\sigma} - h.c. \tag{7}$$

where the unknown coefficients $A^{(s)}_{J\mathbf{k}}$ and $B^{(s)}_{J\mathbf{k}}$ are obtained through the equation $[H_0, S] = H_{hyb}$ and the solution is computed in Appendix and reads

$$A^{(s)}_{J\mathbf{k}\sigma} = \frac{\overline{V}^{(s)}_{J\mathbf{k}\sigma}}{(\epsilon_0 - s\epsilon_{k\sigma})} \qquad B^{(s)}_{J\mathbf{k}\sigma} = -\frac{U\overline{V}^{(s)}_{J\mathbf{k}\sigma}}{(\epsilon_0 - s\epsilon_{k\sigma})(\epsilon_0 + U - s\epsilon_{k\sigma})} \tag{8}$$

By computing $\frac{1}{2}[S, H_{hyb}]$, the transformed Hamiltonian reads

$$H' = H_{sil} + H_U + H''_{sil} + H''_U + H_{dir} + H_{ch} + H_{exch} + H_{hop} \tag{9}$$

where

$$H''_{sil} = \sum_{J,\mathbf{k},\sigma,s}\sum_{\mathbf{k}',s'}A^{(s)}_{J\mathbf{k}\sigma}\overline{V}^{(s')*}_{J\mathbf{k}'\sigma}c^{(s)\dagger}_{\mathbf{k}\sigma}c^{(s')}_{\mathbf{k}',\sigma} \qquad H''_U = \sum_{J,\mathbf{k},\sigma,s}\overline{V}^{(s)*}_{J\mathbf{k}\sigma}\left(A^{(s)}_{J\mathbf{k}\sigma} - B^{(s)}_{J\mathbf{k}\sigma}n_{J-\sigma}\right)f^{\dagger}_{J\sigma}f_{J\sigma} \tag{10}$$

are corrections to the non-interacting Hamiltonian H_0,

$$H_{dir} = \sum_{J,\mathbf{k},\sigma,s}\sum_{\mathbf{k}',s'}\frac{B^{(s)}_{J\mathbf{k}\sigma}}{\sqrt{2}}\frac{\overline{V}^{(s')*}_{J\mathbf{k}'\sigma}}{2}c^{(s)\dagger}_{\mathbf{k}\sigma}c^{(s')}_{\mathbf{k}',\sigma}(n_{J-\sigma} + n_{J\sigma}) \tag{11}$$

$$H_{exch} = \sum_{J,\mathbf{k},\sigma,s}\sum_{\mathbf{k}',s'}\frac{B^{(s)}_{J\mathbf{k}\sigma}}{\sqrt{2}}\left(\frac{\overline{V}^{(s')*}_{J\mathbf{k}'\sigma}}{2}(n_{J\sigma} - n_{J-\sigma})c^{(s)\dagger}_{\mathbf{k}\sigma}c^{(s')}_{\mathbf{k}',\sigma} + \overline{V}^{(s')*}_{J\mathbf{k}'-\sigma}c^{(s')}_{\mathbf{k}',-\sigma}c^{(s)\dagger}_{\mathbf{k}\sigma}f^{\dagger}_{J-\sigma}f_{J\sigma}\right)$$

are the direct (spin-independent) and exchange interaction and

$$H_{ch} = -\sum_{J,\mathbf{k},\sigma,s}\sum_{\mathbf{k}',s'}B^{(s)}_{J\mathbf{k}\sigma}\overline{V}^{(s)}_{J\mathbf{k}'\sigma}c^{(s')\dagger}_{\mathbf{k}',-\sigma}c^{(s)\dagger}_{\mathbf{k}\sigma}f_{J-\sigma}f_{J\sigma} + h.c. \tag{12}$$

is a pair-tunneling term. Finally,

$$H_{hop} = \sum_{J,J'\neq j,\mathbf{k},\sigma,s}\overline{V}^{*(s)}_{J'\mathbf{k}\sigma}(A^{(s)}_{J\mathbf{k}\sigma} - B^{(s)}_{J\mathbf{k}\sigma}n_{J-\sigma})f^{\dagger}_{J'\sigma}f_{J\sigma} + h.c. \tag{13}$$

is an indirect hopping between the magnetic impurities. We can note that if $\lambda = 0$, then $\chi^{(s)}_{k\sigma}$ no longer depends on σ and then H_{sil}, H_U, H_{dir} and H_{exch} can be reduced to the well known results (see

4

eq.(7.122) to eq.(7.127) of [40])

$$H''_{sil} = \sum_{\mathbf{k},\mathbf{k}',s,s'} W^{(s)}_{\mathbf{k}\mathbf{k}'} \psi^{(s)\dagger}_{\mathbf{k}} \psi^{(s')}_{\mathbf{k}'} \qquad H''_U = \sum_{J,\mathbf{k},\sigma,s} (W^{(s)}_{\mathbf{k}\mathbf{k}} - J^{(s)}_{\mathbf{k}\mathbf{k}} n_{J-\sigma}) n_{J\sigma} \qquad (14)$$

$$H_{dir} = \frac{1}{2} \sum_{J,\mathbf{k},\mathbf{k}',s,s'} J^{(s)}_{\mathbf{k}\mathbf{k}'} (\psi^\dagger_J \psi_J)(\psi^{(s)\dagger}_{\mathbf{k}} \psi^{(s')}_{\mathbf{k}'}) \qquad H_{exch} = -\frac{1}{2} \sum_{J,\mathbf{k},\mathbf{k}',s,s'} J^{(s)}_{\mathbf{k}\mathbf{k}'} (\psi^\dagger_J \sigma \psi_J) \cdot (\psi^{(s)\dagger}_{\mathbf{k}} \sigma \psi^{(s')}_{\mathbf{k}'})$$

where the coefficients $W^{(s)}_{\mathbf{k}\mathbf{k}'}$ and $J^{(s)}_{\mathbf{k}\mathbf{k}'}$ read

$$W^{(s)}_{\mathbf{k}\mathbf{k}'} = \sum_{J=1,2} (\overline{V}^{(s)*}_{J\mathbf{k}'} A^{(s)}_{J\mathbf{k}} + \overline{V}^{(s)}_{J\mathbf{k}'} A^{(s)*}_{J\mathbf{k}}) \qquad J^{(s)}_{\mathbf{k}\mathbf{k}'} = \sum_{J=1,2} (\overline{V}^{(s)*}_{J\mathbf{k}'} B^{(s)}_{J\mathbf{k}} + \overline{V}^{(s)}_{J\mathbf{k}'} B^{(s)*}_{J\mathbf{k}}) \qquad (15)$$

where $\psi^{(s)}_{\mathbf{k}} = \binom{c^{(s)}_{\mathbf{k}\uparrow}}{c^{(s)}_{\mathbf{k}\downarrow}}$ and $\psi_J = \binom{f_{J\uparrow}}{f_{J\downarrow}}$ are the two-component spinor operators that remove electrons from the conduction states and from the impurity. In the last equation, $J^{(s)}_{\mathbf{k}\mathbf{k}'}$ is the Kondo coupling which allows for non-trivial effects in the static properties where a resonance in the local density of states at the Fermi level appears [41]. In silicene, not much is known about the experimental spectral features of the Kondo effect although density functional theory has been applied ([42], [43], [44] and [45]) showing that silicene is able to form strong bonds with transition metals due to its buckled structure. The 4th order expansion of the Schrieffer-Wolff transformation give rises to the RKKY interaction which can be obtained as an effective exchange interaction induced by the hybridization of the two local magnetic impurities with the conduction band. In this work, we will focus on the hopping term between impurities that can be written in a more suitable form as

$$H_{hop} = \sum_{\sigma} (T_\sigma f^\dagger_{1\sigma} f_{2\sigma} + T^*_\sigma f^\dagger_{2\sigma} f_{1\sigma}) \qquad (16)$$

$$- \sum_{\sigma} \left[\overline{T}_\sigma (n_{2-\sigma} + n_{1-\sigma}) f^\dagger_{1\sigma} f_{2\sigma} + \overline{T}^*_\sigma (n_{1-\sigma} + n_{2-\sigma}) f^\dagger_{2\sigma} f_{1\sigma} \right]$$

where

$$T_\sigma(\mathbf{R}_1 - \mathbf{R}_2) = \sum_{\mathbf{k},s} (\overline{V}^{*(s)}_{1\mathbf{k}\sigma} A^{(s)}_{2\mathbf{k}\sigma} + \overline{V}^{(s)}_{2\mathbf{k}\sigma} A^{*(s)}_{1\mathbf{k}\sigma}) \qquad (17)$$

$$= \frac{2V^2}{N} (\epsilon_0 + \Delta_\sigma) \sum_{\mathbf{k}} \frac{e^{-i\mathbf{k}\cdot(\mathbf{R}_1 - \mathbf{R}_2)}}{\epsilon_0^2 - \epsilon_{k\sigma}^2}$$

and

$$\overline{T}_\sigma(\mathbf{R}_1 - \mathbf{R}_2) = \sum_{\mathbf{k},s} \overline{V}^{(s)*}_{1\mathbf{k}\sigma} B^{(s)}_{2\mathbf{k}\sigma} = -\frac{V^2 U}{N} \sum_{\mathbf{k}} \frac{U(\epsilon_0 + \Delta_\sigma) + \epsilon_0(\epsilon_0 + 2\Delta_\sigma) + \epsilon_{k\sigma}^2}{(\epsilon_0^2 - \epsilon_{k\sigma}^2)(U^2 + 2U\epsilon_0 + \epsilon_0^2 - \epsilon_{k\sigma}^2)} e^{-i\mathbf{k}\cdot(\mathbf{R}_1 - \mathbf{R}_2)} \qquad (18)$$

are the amplitudes for the effective hopping of the magnetic impurities. A simple inspection of eq.(17) and eq.(18) can be done by considering that in the vicinity of the Fermi level, $k \sim k_F \sim 0$ then

$$T_\sigma = \frac{2V^2}{\epsilon_0 - \Delta_\sigma} \qquad \overline{T}_\sigma = -\frac{UV^2}{(\epsilon_0 - \Delta_\sigma)(\epsilon_0 - \Delta_\sigma + U)} \qquad (19)$$

where the signatures of the quantum-spin Hall phase to quantum-valley Hall phase transition appear in the poles of T_σ and $\overline{T}_\sigma$. The spin-polarized effective electron hopping between impurities obtained generalizes the model considered in [28] and [46] used in graphene, where the hopping between impurities is constant. In figure 2 the effective hoppings are shown as a function of V_z for typical values obtained
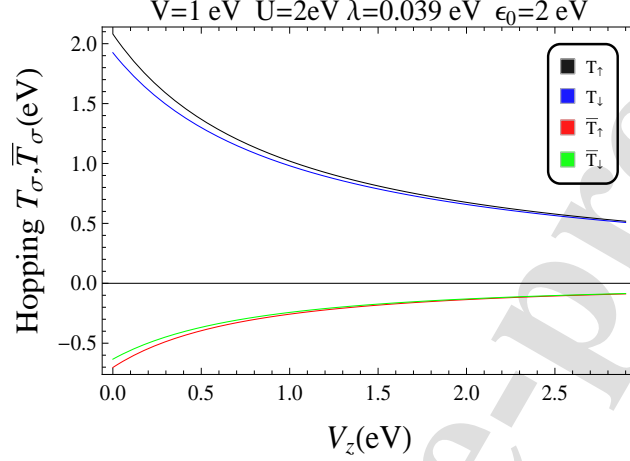
5

Figure 2: Effective hopping as a function of the electric potential at the Dirac point.

from DFT+U (see [48] and [49]) $V = 1$eV, $U = 1$eV and $\epsilon_0 = 2$eV for electrons near the Dirac point where it can be seen that effective hopping is positive when both impurities are empty and is negative when the impurities are occupied. The difference between the spin polarized hopping is larger for $\overline{T}_\sigma$ due to an enhancement of the Hubbard parameter and this favours the formation of ferromagnetic or antifferomagnetic order but this competes with the kinetic energy cost of single occupation of conduction electron levels [47].

3 Results and discussions

In order to analyze the effective hopping between magnetic impurities as a function of the distance we can consider eq.(17) and eq.(18) as a function of the distance between impurities

$$T_\sigma(r) = \gamma \left(\epsilon_0 + \Delta_\sigma \right) \int_0^D \frac{\epsilon}{\epsilon_0^2 - \Delta_\sigma^2 - \epsilon^2} J_0(\epsilon \frac{r}{\hbar v_F}) d\epsilon \tag{20}$$

$$\overline{T}_\sigma(r) = -\gamma \frac{U}{2} \int_0^D \frac{\omega \left(\epsilon_0(\epsilon_0 + U) + (2\epsilon_0 + U)\Delta_\sigma + \epsilon^2 + \Delta_\sigma^2 \right)}{(\epsilon_0^2 - \epsilon^2 - \Delta_\sigma^2) \left((\epsilon_0 + U)^2 - \epsilon^2 - \Delta_\sigma^2 \right)} J_0(\epsilon \frac{r}{\hbar v_F}) d\epsilon$$

where $D \sim 7$eV is the cutoff in energy, $r = |\Delta \mathbf{R}|$ is the inter-impuritiy distance, $n = N/A$ is the areal density of the host lattice and A is the silicene area, $\epsilon = \hbar v_F k$ and $J_0(x)$ is the Bessel function of the first kind. Both integrals can be solved numerically and the dependence of T_σ and $\overline{T}_\sigma$ with r is shown for particular values of ϵ_0, U and V_z in figure 3, where the dimensionless constant $\gamma = \frac{V^2}{n\pi(\hbar v_F)^2} \sim 0.24$ is used for $V = 1$eV and $A = \frac{\sqrt{3}}{2}a^2$, where $a = 3.86$Å. From eq.(16) we can note that the impurity positions appear in T_σ and $\overline{T}_\sigma$ through terms that depend on $V_{1\mathbf{k}\sigma}^* V_{2\mathbf{k}\sigma}$ which gives a $\mathbf{R}_1 - \mathbf{R}_2$ dependence. In turn, when the $\mathbf{k}$ integral is computed, the Fourier transform of $\frac{1}{\epsilon_0^2 - \hbar^2 v_F^2 k^2 - \Delta_\sigma^2}$ is obtained, which is isotropic in $\mathbf{k}$ space and consequently an isotropic spatial dependence of T_σ and $\overline{T}_\sigma$ is obtained. It should be stressed that the expression of eq.(20) is valid in the long-wavelength limit for distances larger than the lattice constant. In silicene $a = 3.86$Å$= 0.386$nm. Then the limit of validity of eq.(20) is $r > 0.386$nm. The relative distance between impurities is identical if both are in the A sublattice or B sublattice. When both impurities are located in different sublattices, we must replace $\mathbf{R}_1 - \mathbf{R}_2$ by $\mathbf{R}_1 - \mathbf{R}_2 + \delta_1$ in the results obtained, which implies that the plots of T_σ and $\overline{T}_\sigma$ as a function of r

6

are shifted by $|\delta_1|$ when both impurities are located in different sublattices. There is a negligible spin polarization in T_σ as a function of r when the impurities are not occupied but changes subtantially when the Hubbard term becomes more relevant as it can be seen in figure (3 left). An interesting behavior can be seen in the regions of r where $\overline{T}_\uparrow$ and $\overline{T}_\downarrow$ are zero because in these regions $\overline{T}_\uparrow = -\overline{T}_\downarrow$, which indicates that a particular spin effective hopping is energetically favored and this behavior is enhanced for higher U. This result implies that the precursor of RKKY interaction allows a reversible switching between ferromagnetic and anti-ferromagnetic exchange interactions, upon changing the impurity distances [50]. Moreover, the spin polarized distance dependence of the effective tunneling terms $\overline{T}_\sigma(r)$ implies that the impurity spin-spin correlation function decays remarkably slower than the textbook expression of the RKKY interaction, even for a finite bandwidth of the conduction band. By restricting the
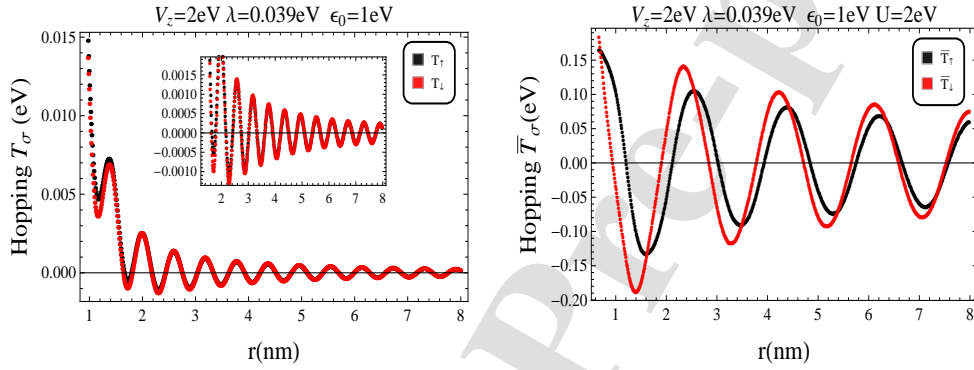

Figure 3: Effective hopping as a function of the distance $r = |\Delta \mathbf{R}|$ between magnetic impurities. Left: Hopping channel when the magnetic adatoms are empty. Right: Hopping channel when at least a magnetic adatom is singly occupied.

Hamiltonian H' to the impurity sector $H_{\rm imp} = H_U + H_U'' + H_{hop}$, we obtain a two-site Hubbard model with electron hopping between magnetic impurities induced by the host lattice. Each lattice site may be either empty, occupied by an electron of spin up or down, or doubly occupied. The Hilbert space of the two-site Hubbard model has a dimension of $2^4 = 16$. Because $[H_{\rm imp}, N] = 0$, the full space H decomposes as a direct sum of subspaces of fixed particle number, so that we can avoid 16×16 matrices by working in sectors of fixed particle number. The most important sector is the 2-site model because it describes half filling and the one-dimensional subspaces with $N = 0$ and $N = 4$ electrons have no dynamics. For a detailed analysis, we can apply a projector $\Pi_{\rm 1P}$ onto the single–occupancy sector for the two local magnetic states

$$\Pi_{\rm 1P} = \sum_\sigma n_{1\sigma}(1 - n_{2\uparrow}n_{2\downarrow}) + \sum_\sigma n_{2\sigma}(1 - n_{1\uparrow}n_{1\downarrow}) - 2\sum_{J,\sigma} n_{J\sigma}n_{J-\sigma} - 2\sum_\sigma n_{1\sigma}n_{2\sigma} + 4n_{1\uparrow}n_{1\downarrow}n_{2\uparrow}n_{2\downarrow} \quad (21)$$

which obey $\Pi_{\rm 1P} H_{\rm Imp} \Pi_{\rm 1P} = H_{\rm Imp} \Pi_{\rm 1P}$. The projector $\Pi_{\rm 1P}$ projects out states without one occupancy. Similarly, we can define projectors onto sectors with double, tripe and quadruple occupation, as follows

$$\Pi_{\rm 2P} = n_{1\uparrow}n_{1\downarrow}(1 - 3(n_{2\uparrow} + n_{2\downarrow})) + n_{2\uparrow}n_{2\downarrow}(1 - 3(n_{1\uparrow} + n_{1\downarrow})) + (n_{1\uparrow} + n_{1\downarrow})(n_{2\uparrow} + n_{2\downarrow}) + 6n_{1\uparrow}n_{1\downarrow}n_{2\uparrow}n_{2\downarrow} \quad (22)$$

$$\Pi_{\rm 3P} = n_{1\uparrow}n_{1\downarrow}(n_{2\uparrow} + n_{2\downarrow}) + n_{2\uparrow}n_{2\downarrow}(n_{1\uparrow} + n_{1\downarrow}) - 4n_{1\uparrow}n_{1\downarrow}n_{2\uparrow}n_{2\downarrow}$$
$$\Pi_{\rm 4P} = n_{1\uparrow}n_{1\downarrow}n_{2\uparrow}n_{2\downarrow}$$

The set of projectors obey $\Pi_{J{\rm P}}\Pi_{J'{\rm P}} = \Pi_{J{\rm P}}\delta_{JJ'}$. In the one-electron sector the $H_{\rm imp}\Pi_{\rm 1P}$ reads

$$H_{\rm imp}\Pi_{\rm 1P} = \sum_{j,\sigma} \epsilon_\sigma f_{j\sigma}^\dagger f_{j\sigma} + \sum_\sigma (T_\sigma f_{1\sigma}^\dagger f_{2\sigma} + T_\sigma^* f_{2\sigma}^\dagger f_{1\sigma}) \quad (23)$$
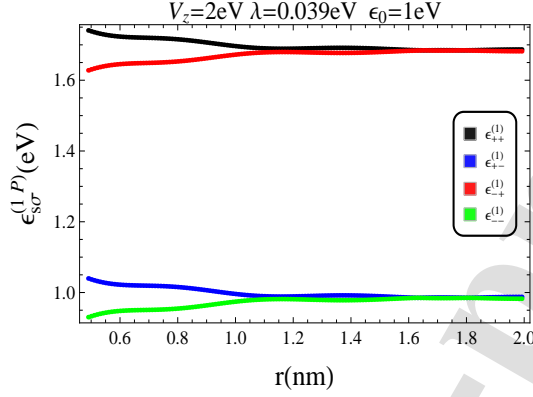
7

Figure 4: Spectrum of the two-site Hubbard model for single occupancy as a function of the distance $|\Delta\mathbf{R}|$ between magnetic adatoms.

where $\epsilon_\sigma = \epsilon_0 + T_\sigma^{(0)}$ is the effective on-site energy of the impurity and $T_\sigma^{(0)} = T_\sigma(0)$. The normalization introduces a spin-dependent on-site energy. The eigenvalues of eq.(23) read

$$\epsilon_{s\sigma}^{(1\mathrm{P})} = \epsilon_\sigma + s\,|T_\sigma| = \epsilon_0 + \frac{2V^2}{\epsilon_0 - \Delta_\sigma} + s\left|\frac{2V^2}{\epsilon_0 - \Delta_\sigma}\right| \tag{24}$$

with $s, \sigma = \pm 1$. The associated eigenvectors are $|\phi_{s\sigma}\rangle = \frac{1}{\sqrt{2}}(s\,|\sigma, 0\rangle + |0, \sigma\rangle)$. As it can be seen in figure 4, the lowest eigenvalue is $\epsilon_{--}^{(1\mathrm{P})}$ and the electron is shared between the impurities in a superposition $|\phi_{--}\rangle = \frac{1}{\sqrt{2}}(-|\downarrow, 0\rangle + |0, \downarrow\rangle)$. For large r, $\epsilon_{++}^{(1\mathrm{P})} = \epsilon_{-+}^{(1\mathrm{P})}$ and $\epsilon_{--}^{(1\mathrm{P})} = \epsilon_{+-}^{(1\mathrm{P})}$ which indicates a transition to a degenerated ground state. The $H_{\mathrm{imp}}\Pi_{2\mathrm{P}}$ in the 2-electron sector reads

$$H_{\mathrm{imp}}\Pi_{2\mathrm{P}} = 2\epsilon_0 \sum_\sigma n_{1\sigma} n_{2\sigma} + (2\epsilon_0 + L) \sum_\sigma n_{1\sigma} n_{2-\sigma} + (2\epsilon_0 + U + L - \overline{L}) \sum_J n_{J\uparrow} n_{J\downarrow} \tag{25}$$

$$+ \sum_\sigma (T_\sigma^{(0)} - T_\sigma)(n_{1-\sigma} f_{1\sigma}^\dagger f_{2\sigma} + n_{2-\sigma} f_{1\sigma}^\dagger f_{2\sigma}) + \sum_\sigma (T_\sigma^{(0)} - T_\sigma^*)(n_{2-\sigma} f_{2\sigma}^\dagger f_{1\sigma} + n_{1-\sigma} f_{2\sigma}^\dagger f_{1\sigma})$$

that decouples the parallel spin eigenstates with $s_z = \pm 1$ eigenvalues from the anti-parallel $S_z = 0$ sector given by $\{|\uparrow, \downarrow\rangle, |\downarrow, \uparrow\rangle, |\uparrow\downarrow, 0\rangle, |0, \uparrow\downarrow\rangle\}$ with total spin $s_z = 0$ eigenvalues. The eigenvalues of the spin-parallel sector are $\epsilon_\sigma^{(2, s_z = \pm 1)} = 2(\epsilon_0 + T_\sigma^{(0)})$ and do not depend on the distance between impurities because parallel spins in different adatoms cannot tunnel due to the exclusion principle. The eigenvalues of the $S_z = 0$ spin sector read

$$\epsilon_{s\sigma}^{(2, s_z = 0)} = \frac{1}{2}(U - \overline{L} + 4\epsilon_0 + 2T_\sigma^{(0)}) + \frac{s}{2}\sqrt{(U - \overline{L})^2 + 4(\left|T_\uparrow^{(0)} - T_\uparrow^*\right| + \sigma\left|T_\downarrow^{(0)} - T_\downarrow^*\right|)^2} \tag{26}$$

where $L = \sum_\sigma T_\sigma^{(0)}$, $\overline{L} = 2\sum_\sigma \overline{T}_\sigma^{(0)}$. For $\mathbf{k} \sim 0$, $T_\sigma^{(0)} - T_\sigma^* = 0$ and

$$\lim_{\mathbf{k} \to 0} \epsilon_{s\sigma}^{(2, s_z = 0)} = \frac{1}{2}U + 2\epsilon_0 + \frac{V^2(U + 2(\epsilon_0 - \Delta_\sigma))}{(\epsilon_0 - \Delta_\sigma)(U + \epsilon_0 - \Delta_\sigma)} \tag{27}$$

$$+ \frac{sU}{2}\left|1 + \frac{2V^2}{(\epsilon_0 - \Delta_\sigma)(U + \epsilon_0 - \Delta_\sigma)}\right|$$

8

From the last equation, when U becomes large, there are only two levels ($\epsilon_{-+}^{(2,s_z=0)}$ and $\epsilon_{--}^{(2,s_z=0)}$) with energy close to zero that have mainly covalent character at the Dirac point. For arbitrary values of $\mathbf{k}$ the $\epsilon_{s\sigma}^{(2,s_z=0)}$ energy levels are shown in figure 5 as a function of the inter-impurity distance for different values of V_z and for $U = 2$eV, where it can be seen that for $V_z = 0.6$eV the ground state is degenerated for critical r values and the two eigenvalues with $\sigma = -1$ are no longer constant as a function of r. The $\epsilon_{+-}^{(2,s_z=0)}$ and $\epsilon_{--}^{(2,s_z=0)}$ eigenstates do not depend on the distance between impurities for $V_z < 0.6$eV due to the negligible difference between $\left|T_\uparrow^{(0)} - T_\uparrow^*\right|$ and $\left|T_\downarrow^{(0)} - T_\uparrow^*\right|$. The lowest level corresponds to an eigenstate

$$\left|\phi_{-+}^{(2P)}\right\rangle = \frac{1}{\sqrt{2(|a|^2 + 1)}} \left[a(|\uparrow, \downarrow\rangle + |\downarrow, \uparrow\rangle) + |\uparrow\downarrow, 0\rangle + |0, \uparrow\downarrow\rangle\right] \tag{28}$$

where

$$a(r) = -\sqrt{\frac{T_\uparrow^{(0)} + T_\uparrow}{T_\uparrow^{(0)} + T_\uparrow^*}} \left(\frac{U - \overline{L} + \epsilon_0 - \epsilon_{-+}^{(2P\ s_z=0)}}{\left|T_\downarrow^{(0)} + T_\downarrow\right| + \left|T_\uparrow^{(0)} + T_\uparrow\right|}\right) \tag{29}$$

The state $\left|\phi_{-+}^{(2P)}\right\rangle$ contains an admixture of the superpositions $|\uparrow, \downarrow\rangle$, $|\downarrow, \uparrow\rangle$, $|\uparrow\downarrow, 0\rangle$, $|0, \uparrow\downarrow\rangle$ whose relative proportions are fixed by $a(r)$ as it is shown in figure (6), where $\left|(\langle\uparrow, \downarrow| + \langle\downarrow, \uparrow|)\left|\phi_{-+}^{(2P)}\right\rangle\right|^2$ and $\left|(\langle\uparrow\downarrow, 0| + \langle 0, \uparrow\downarrow|)\left|\phi_{-+}^{(2P)}\right\rangle\right|^2$ is plotted agains r for different values of V_z with $V = 1$eV, $\epsilon_0 = 1$eV and $U = 2$eV. For a vanishing applied electric field, the state $\left|\phi_{-+}^{(2P)}\right\rangle$ is mostly an ionic state and only
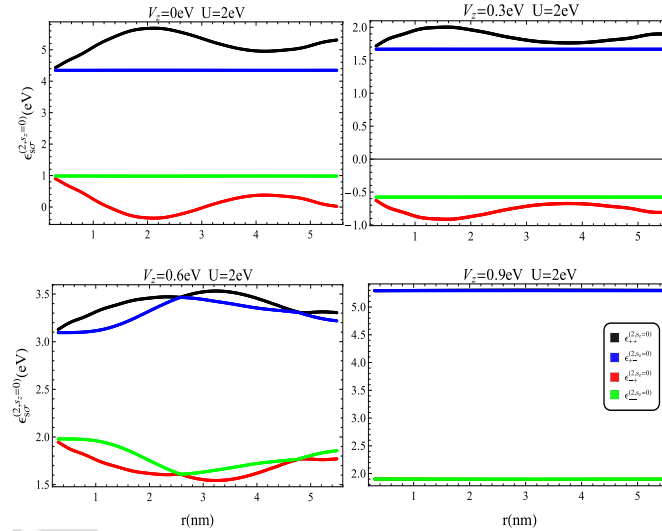

Figure 5: Spectrum for double occupancy with total spin $s_z = 0$ as a function of the distance for different values of V_z and $U = 2$eV, $V = 1$eV and $\epsilon_0 = 1$eV.

identical contributions are obtained for $|\Delta\mathbf{R}| \to 0$, where the local orbitals start to overlap at short distances and form dimers [51]. By increasing V_z to 0.3eV, a transition to a covalent ground state $\left|\phi_{-+}^{(2P)}\right\rangle$ is obtained for the whole domain studied for r. When $V_z > 0.6$eV the ground state returns to the ionic phase and for $V_z = 0.6$eV and for 2nm$< r <$ 3.5nm we obtain a region where the ground state is mostly ionic but it can be transformed to a covalent state by altering the local position of

9

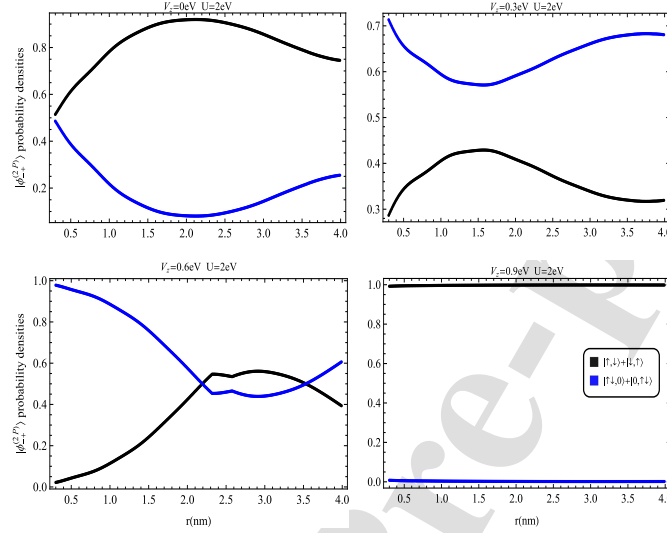one impurity. This critical behavior of the ground state with one electron per-site as a function of the

Figure 6: Relative weights of the ionic and covalent states on the ground state with double occupancy for different values of V_z with $U = 2$eV, $V = 1$eV and $\epsilon_0 = 1$eV.

applied external electric field is conducive to entanglement generation between localized states in the impurities with a vanishing net magnetization with the specific Hamiltonian parameters used. This entanglement is obtained when a free electron moving through the lattice impinges on two magnetic impurities [52]. The 3-particle subspace is composed of states with two spins paired on a site and one
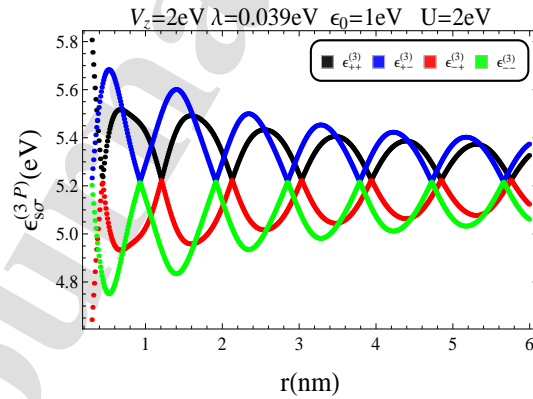

Figure 7: Spectrum of the two-site Hubbard model in silicene with triple occupancy.

spin unpaired. The basis for this space can thus be labeled by the position and spin of the isolated electron, making it isomorphic to the $N = 1$ subspace [53]. In the triple-occupance sector, $H_{\text{imp}}\Pi_{3P}$

10

reads

$$H_{\text{imp}}\Pi_{3P} = \sum_\sigma (2\epsilon_0 + U + R_\sigma)n_{1\uparrow}n_{1\downarrow}n_{2\sigma} + \sum_\sigma (2\epsilon_0 + U + R_\sigma)n_{2\uparrow}n_{2\downarrow}n_{1\sigma} \tag{30}$$

$$+ \sum_\sigma (T_\sigma^* - 2\overline{T}_\sigma^*)n_{1-\sigma}n_{2-\sigma}f_{2\sigma}^\dagger f_{1\sigma} + \sum_\sigma (T_\sigma - 2\overline{T}_\sigma)n_{1-\sigma}n_{2-\sigma}f_{1\sigma}^\dagger f_{2\sigma}$$

where $R_\sigma = T_\sigma^{(0)} + \frac{1}{2}T_{-\sigma}^{(0)} - \frac{\overline{L}}{2}$ and the eigenvalues read

$$\epsilon_{s\sigma}^{(3P)} = 2\epsilon_0 + U + R_\sigma + s\left|T_{-\sigma} - 2\overline{T}_{-\sigma}\right| \tag{31}$$

By comparing with eq.(24), the renormalization of the on-site energy of the impurities acquires a U and r dependence. The energy levels come closer to each other for large distances and the ground state is given by $\epsilon_{--}^{(3P)}$ as it can be seen in figure 7. This result is in concordance with the ground state of the single-occupancy sector for the same parameters. The 4-particle subspace is one dimensional and the energy is $\epsilon^{(4P)} = 4\epsilon_0 + 2U + \sum_\sigma(\frac{1}{2}T_\sigma^{(0)} - \overline{T}_\sigma^{(0)})$ and does not depend on the distance. In order to analyze the average occupation number, we can decompose the full Hilbert space $\mathcal{H}$ as a direct sum of subspaces of fixed particle number $\mathcal{H} = \mathcal{H}_0 \otimes \mathcal{H}_1 \otimes \mathcal{H}_2 \otimes \mathcal{H}_3 \otimes \mathcal{H}_4$, the partition function can be written as $Z = \sum_{j=0}^{4} Z_j$ where $Z_j = \sum_\alpha e^{-\beta\epsilon_\alpha^{(j)}}$ and the average number occupation can be computed as

$$N_{\text{ave}} = \frac{1}{Z}\sum_\alpha^4 N_\alpha e^{-\beta E_\alpha} = \frac{Z_1 + 2Z_2 + 3Z_3 + 4Z_4}{Z_0 + Z_1 + Z_2 + Z_3 + Z_4} \tag{32}$$
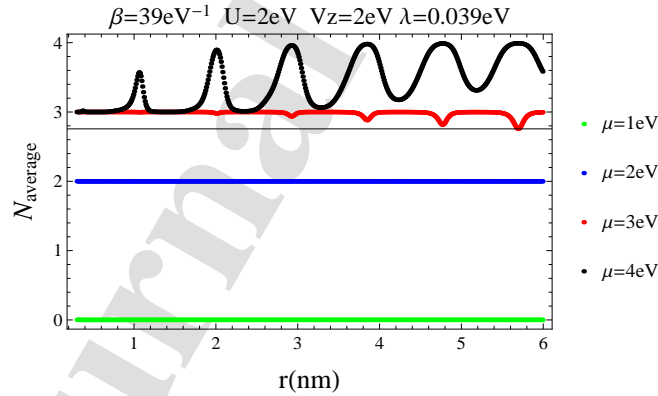

Figure 8: Average number occupation for the two-site Hubbard model for different temperatures $\beta = 1/kT$.

Figure 8 shows N as function of r for various values of Fermi level μ and for $\beta = 39\text{eV}^{-1}$ which corresponds to $T = 300$K. For $\mu \geq 2$eV the N_{ave} shows clearly visible Mott plateaus at different values of r. These plateaus form a pattern with dips for $\mu = 3$eV and hills for $\mu = 4$eV, at those points in r at which $T_\uparrow$ and $T_\downarrow$ have opposite signs. Changing β washes out or sharpens the features discussed above. These results are important for studying the Kondo regime of TIAM in silicene with spin-orbit coupling. It has been shown that for a Hamiltonian with spin-flip symmetry, a competition between antiferromagnetic (AF) and Kondo physics take place, but for large β and relatively small distances between impurities, the AF splitting dominates and the local moment of the impurities is frozen and

11

is independent of the distance. On the opposite end, for large distances, the AF gap allows the Kondo regime to take place [54]. This analysis no longer holds because the precursor of the RKKY interaction obtained in eq.(9) allows a certain set of Hamiltonian parameters and impurity configurations for which the effective hopping is positive for one spin value and negative for the other. This unusual behavior causes a twisted exchange interaction between adsorbed magnetic moments where the tunability of the RKKY terms using a perpendicular electric field and varying the Fermi energy is possible [55]. Finally, it should be stressed that the effective hopping obtained in eq.(16) implies that the distance between impurities is critical for studying the formation of local magnetic moments as it has been done in [28] and [29]. When the mean field approximation [22] is considered, we must replace $U n_\uparrow n_\downarrow = U \sum_s \epsilon_s n_s$, where $\epsilon_s = \epsilon_0 + U \langle n_{-s} \rangle$ is the effective on-site energy of an impurity and where a constant term $-U \langle n_\uparrow \rangle \langle n_\downarrow \rangle$ can be dropped. Under this approximation, the impurity Hamiltonian H_{Imp} can be written as

$$H = \left(\begin{array}{cccc} f_{1\uparrow}^\dagger & f_{1\downarrow}^\dagger & f_{2\uparrow}^\dagger & f_{2\downarrow}^\dagger \end{array} \right) \times \tag{33}$$

$$\left(\begin{array}{cccc} \epsilon_\uparrow + U_\uparrow \langle n_{1\downarrow} \rangle & 0 & T_\uparrow^* - \overline{T}_\uparrow^* \langle n_\downarrow \rangle & 0 \\ 0 & \epsilon_\downarrow + U_\downarrow \langle n_{1\uparrow} \rangle & 0 & T_\downarrow^* - \overline{T}_\downarrow^* \langle n_\uparrow \rangle \\ T_\uparrow - \overline{T}_\uparrow \langle n_\downarrow \rangle & 0 & \epsilon_\uparrow + U_\uparrow \langle n_{2\downarrow} \rangle & 0 \\ 0 & T_\downarrow - \overline{T}_\downarrow \langle n_\uparrow \rangle & 0 & \epsilon_\downarrow + U_\downarrow \langle n_{2\uparrow} \rangle \end{array} \right) \left(\begin{array}{c} f_{1\uparrow} \\ f_{1\downarrow} \\ f_{2\uparrow} \\ f_{2\downarrow} \end{array} \right)$$

where $\langle n_\sigma \rangle = \langle n_{1\sigma} \rangle + \langle n_{2\sigma} \rangle$, $\epsilon_\sigma = \epsilon_0 - \frac{T_\sigma^{(0)}}{2}$ and $U_\sigma = \frac{U}{2} - \overline{T}_\sigma^{(0)}$. A simple inspection indicates that the hybridization between the impurities contains contributions from the mean value of the occupation numbers and these contributions are not taken into account in [28] and [29] (see eq.(8) and eq.(4) respectively). In turn, for small values of r, $T_\uparrow \neq T_\downarrow$ (see figure 3), which implies that, even without considering the effects of the occupation numbers, the hopping channel between impurities is asymmetric with respect to the spin. For example, with $V = 1$eV, $\epsilon_0 = 2$eV, $\lambda = 39$meV and $V_z = 2$eV and $r = 0.3$nm, $T_\uparrow = 0.669$eV and $T_\downarrow = 0.685$eV and for $r = 1$nm, $T_\uparrow = 0.049$eV and $T_\downarrow = 0.044$eV. The spin-asymmetric interaction between the impurities should modify the symmetry of the boundary of the magnetic phase diagrams of figure 5 of [29].

4   Conclusions

In this work we have studied the effective hybridization between two magnetic impurities placed in the A sublattice of silicene. By considering a perpendicular electric field and a spin-orbit coupling, we obtain an effective hopping term between impurities by applying the Schrieffer-Wolff transformation. This hopping depends on the distance between the magnetic adatoms and is different when these impurities are empty or occupied. By restricting to the impurity Hilbert space, we study the eigenvalues and eigenvectors of the impurity Hamiltonian for different occupation numbers and we show a non-trivial dependence on distance. In particular, at half filling it is possible to find a set of Hamiltonian parameters in which the spin polarized effective hopping has different signs for each spin indicating a privileged spin channel scattering. In turn, a ground state transition from an ionic state to a covalent state and viceversa is obtained by tuning the external electric field and for critical values it is possible to obtain both ground states by altering the local position of the impurities. Finally, we study the average occupation number as a function of the distance between impurities for different Fermi energies, showing the formation of a pattern of Mott plateaus. These results are important for studying the formation of local magnetic moments due to the significant change in the effective hybridization when the magnetic adatoms are occupied or empty. The results obtained are useful to understand how to electrically control the magnetic ground state in nanoelectronic devices based on silicene. 2D materials with buckling give us a platform to design experiments to investigate by using scanning tunneling microscopy to locate impurities on specific positions and then manipulating the hopping term between them by varying the Fermi energy through a gate voltage.

5   Acknowledgment

6   Author contributions

All authors contributed equally to all aspects of this work.

7   Appendix

7.1 S matrix computation

In order to obtain the matrix operator S we can consider the following ansatz for S

$$S = \sum_{J,\mathbf{k},\sigma,s} (A^{(s)}_{J\mathbf{k}\sigma} + B^{(s)}_{J\mathbf{k}\sigma} n_{J-\sigma}) c^{(s)\dagger}_{\mathbf{k}\sigma} f_{J\sigma} - h.c. \tag{34}$$

where $J = 1, 2$ indicates the magnetic impurity, $\mathbf{k}$ is the wave vector, $s = \pm 1$ is the band index and σ is the spin index. The unknown coefficients $A_{j\mathbf{k}}$ and $B_{j\mathbf{k}}$ must be determined through the equation $[H_0, S] = H_{hyb}$. By writing $S = S_1 - S_1^\dagger$ then $[S, H_0] = [S_1, H_0] + [S_1, H_0]^\dagger$ which implies that we only need to compute $[S_1, H_0]$. We can write $H_0 = H_{sil} + H_U + H_{imp}$ and by using $[A, BC] = \{A, B\}C - B\{C, A\}$ and $\left[c^{(s)\dagger}_{\mathbf{k}\sigma}, c^{(s')\dagger}_{\mathbf{k}'\sigma'} c^{(s')}_{\mathbf{k}'\sigma'} \right] = -\delta_{\mathbf{k}\mathbf{k}'} \delta_{\sigma\sigma'} \delta_{ss'} c^{(s')\dagger}_{\mathbf{k}'\sigma'}$, the commutator $[S_1, H_{sil}]$ can be written as

$$[S_1, H_{sil}] = - \sum_{J,\mathbf{k},\sigma,s} s\epsilon_{k\sigma} (A^{(s)}_{J\mathbf{k}\sigma} + B^{(s)}_{J\mathbf{k}\sigma} n_{J-\sigma}) c^{(s)\dagger}_{\mathbf{k}\sigma} f_{J\sigma} \tag{35}$$

In turn, by using $[f_{J\sigma}, n_{J'\sigma'}] = \delta_{JJ'} \delta_{\sigma\sigma'} f_{J'\sigma'}$ and $[f_{J\sigma}, n_{J'\uparrow} n_{J'\downarrow}] = \delta_{JJ'} f_{J'\sigma} n_{J'-\sigma}$ we obtain for the commutator $[S_1, H_U]$

$$[S_1, H_U] = \sum_{J,\mathbf{k},\sigma,s} \epsilon_0 (A^{(s)}_{J\mathbf{k}\sigma} + B^{(s)}_{J\mathbf{k}\sigma} n_{J-\sigma}) c^{(s)\dagger}_{\mathbf{k}\sigma} f_{J\sigma} + \sum_{J,\mathbf{k},\sigma,s} U (A^{(s)}_{J\mathbf{k}\sigma} + B^{(s)}_{J\mathbf{k}\sigma}) n_{J-\sigma} c^{(s)\dagger}_{\mathbf{k}\sigma} f_{J\sigma} \tag{36}$$

Collecting all the terms in $[H_0, S] = H_{hyb}$ we obtain the following solutions for $A^{(s)}_{J\mathbf{k}\sigma}$ and $B^{(s)}_{J\mathbf{k}\sigma}$

$$A^{(s)}_{J\mathbf{k}\sigma} = \frac{\overline{V}^{(s)}_{J\mathbf{k}\sigma}}{(\epsilon_0 - s\epsilon_{k\sigma})} \qquad B^{(s)}_{J\mathbf{k}\sigma} = -\frac{U\overline{V}^{(s)}_{J\mathbf{k}\sigma}}{(\epsilon_0 - s\epsilon_{k\sigma})(\epsilon_0 + U - s\epsilon_{k\sigma})} \tag{37}$$

This result is used in Section II.

References

[1] B. Lalmi, H. Oughaddou, H. Enriquez, A. Kara, S. Vizzini, B. Ealet, and B. Aufray, *Appl. Phys. Lett.* **97**, 223109 (2010).

[2] P. Vogt, P. De Padova, C. Quaresima, J. Avila, E. Frantzeskakis, M. C. Asensio, A. Resta, B. Ealet, and G. Le Lay, *Phys. Rev. Lett.*, **108**, 155501 (2012).

[3] K. Takeda and K. Shiraishi, *Phys. Rev. B* **50**, 14916 (1994).

[4] C. C. Liu, W. Feng, Y. Yao, *Phys. Rev. Lett.*, **107** (7), 076802 (2011).

[5] C. C. Liu, H. Jiang, andY. Yao, *Phys. Rev. B* **84**, 195430 (2011).

[6] M. Ezawa, *New J. Phys.* **14**, 033003 (2012).

[7] P. De Padova, C. Quaresima, C. Ottaviani, P. M. Sheverdyaeva, P. Moras, C. Carbone, D.Topwal, B. Olivieri, A. Kara, H. Oughaddou, B. Aufray, and G. Le Lay, *Appl. Phys. Lett.*, **96**, 261905 (2010).

[8] S. Cahangirov, M. Topsakal, E. Aktürk, H. ̧Sahin, and S. Ciraci, *Phys. Rev. Lett.* **102**, 236804 (2009).

[9] M. Pizzochero, M. Bonfantia, and R. Martinazzo, *Phys. Chem. Chem. Phys.* **18**, 15654 (2016).

[10] Y. Yao, F. Ye, X. L. Qi, S. C. Zhang, Z. Fang, *Phys. Rev. B*, **75** (4) 041401 (2007).

[11] F. Escudero, J. S. Ardenghi and P. Jasen, *Jour. Magn. Magn. Mat.*, **454**, 131-138 (2018).

[12] F. Escudero, J. S. Ardenghi, L. Sourrouille and P. Jasen, *Jour. Magn. Magn. Mat.*, **429**, 294-298 (2017).

[13] F. Escudero, J. S. Ardenghi and P. Jasen, *J. Phys. Condens. Matter*, **31**, 285804 (2019).

[14] D. Loss and D. P. DiVincenzo, *Phys. Rev. A* **57**, 120 (1998).

[15] G. Burkard, D. Loss, and D. P. DiVincenzo, *Phys. Rev. B* **59**, 2070 (1999).

[16] B. A. Trauzettel, D. V. Bulaev, D. Loss, and G. Burkard, *Nature Physics* **3**, 192 (2007).

[17] I. Zutic, J. Fabian, and S. Das Sarma, *Rev. Mod. Phys.* **76**, 323 (2004).

[18] W. Han, R. K. Kawakami, M. Gmitra, and J. Fabian, *Nat Nano* **9**, 794 (2014).

[19] A. Spinelli, M. Gerrits, R. Toskovic, B. Bryant, M. Ternes, and A. F. Otte, *Nature Communications* **6**, 10046 (2015).

[20] O. V. Yazyev and L. Helm, *Phys. Rev. B* **75**, 125408 (2007).

[21] E. Rotenberg, *Graphene Nanoelectronics*, in: H.Raza (Ed.), Springer-Verlag, Berlin, Heidelberg, 2012.

[22] P.W. Anderson, *Phys. Rev.,* **124**, 41 (1964).

[23] S. Alexander, P.W. Anderson, *Phys. Rev.* **133**, A1594 (1964).

[24] J. Villarreal, J. S. Ardenghi and P. Jasen, *Super. and Micro.*, **130** (285-296) 2019.

[25] J. Villarreal, F. Escudero, J. S. Ardenghi and P. Jasen, *Jour. Magn. Magn. Mat.*, **524**, 167598 (2021).

[26] F. Escudero, J. S. Ardenghi, L. Sourrouille, P. Jasen and A. Juan, *Super. and Micro.*, **113**, 291-300 (2018).

[27] P.Venezuela, R. B. Muniz, A. T. Costa, D. M. Edwards, S. R. Power, M. S. Ferreira, *Phys. Rev. B,* **80** 241413 (2009).

[28] Y. Gao, G. Zhou and K.-H. Ding, *Solid State Communications*, **159**, 1-5 (2013).

[29] A. Ghosh, H.O. Frota, . *Jour. Magn. Magn. Mat.*, **454**, 237-242 (2018).

[30] S. LeBohec, J. Talbot, E.J. Mishchenko, Phys. Rev. B 89, 045433 (2014).

[31] M. J. Spencer, T. Morishita (Eds.), *Silicene*, Springer International Publishing, 2016.

[32] M. Laubach, J. Reuther, R. Thomale, S. Rachel, *Phys. Rev. B* **90**, 165136 (2014).

[33] C. L. Kane and E. J. Mele, *Phys. Rev. Lett.,* **95**, 226801 (2005).

[34] F. Parhizgar, H. Rostami, and R. Asgari, *Phys. Rev. B* **87**, 125401 (2013).

[35] Y. Zheng and T. Ando, *Phys. Rev. B* **65**, 245420 (2002).

[36] M. Zare, *Phys. Rev. B* **99**, 235413 (2019).

[37] J.R.Schrieffer and P.A.Wolff, *Phys. Rev.***149**, 2 (1966).

[38] S. Bravyi, D. P. DiVincenzo and D. Loss, *Ann. Phys.*, **326**, 2793 (2011).

[39] P. O. Löwdin, *J. Mol. Spectrosc.*, **10**: 12-33 (1963).

[40] P. Philips, *Advanced solid state physics*, Westview Press (2002).

[41] A. C. Hewson, *The Kondo problem to heavy fermions* (Cambridge University Press, Cambridge, 1997).

[42] B. Aufray, A. Kara, S. Vizzini, H. Oughaddou, C. Léandri, B. Ealet and G. Le Lay, *Appl. Phys. Lett.* **96** 183102 (2010).

[43] E. Cinquanta, E. Scalise, D. Chiappe, C. Grazianetti, B. van den Broek, M. Houssa, M. Fanciulli and A. Molle, *J. Phys. Chem. C*, **117** 16719–24 (2013).

[44] N. Y. Dzade, K. O. Obodo, S. K. Adjokatse, A. C. Ashu, E. Amankwah, C. D. Atiso, A. A. Bello, E. Igumbor, S. B. Nzabarinda, J. T. Obodo, A. O. Ogbuu, O. E. Femi, J. O. Udeigwe and U. V. Waghmare, *J. Phys.: Condens. Matter*, **22** 375502 (2010).

[45] V. Q. Bui, T. T. Pham, H. V. S. Nguyen and H. Le, *J. Phys. Chem. C*, **117** 23364–71 (2013).

[46] A. Ghosh, H.O. Frota, *Physica B,* **407** 1170 (2012).

[47] D. C. Mattis, *The Theory of Magnetism Made Simple*, (World Scientific, Singapore), 2004.

[48] M. Yu, S. Yang, C. Wu, N. Maron, *npj Computational Materials*, **6**:180 (2020).

[49] B. Uchoa, V. N. Kotov, N. M. R. Peres and A. H. Castro Neto, *PRL*, **101**, 026805 (2008).

[50] D. Badrtdinov, A. N. Rudenko, M. I. Katsnelson and V. V. Mazurenko, *2D Materials*, **7** 4 (2020).

[51] T. Esat, B. Lechtenberg, T. Deilmann, C. Wagner, P. Kruger, R. Temirov, M. Rohlfing, F. B. Anders, and F. S. Tautz, *Nat. Phys.*, **12** (2016).

[52] M. Amini, M. Soltani, E. Ghanbari-Adivi and M. Sharbafiun, *Quantum Information Processing* **18**, 78 (2019).

[53] F. H.L. Essler, H. Frahm, F. Göhmann, A. Klümper, and V. E. Korepin. *The One-Dimensional Hubbard Model.* (Cambridge University Press, 2005).

[54] R. Allub, *J. Phys.: Condens. Matter*, **20** 44 (2008).

[55] M. Zare, *Phys. Rev. B* **100**, 085434 (2019).

Highlights:

- Two magnetic impurities located in the A sublattices are studied in silicene subject to an external electric field by applying the Schrieffer-Wolff transformation.
- Hopping terms between impurities are analyzed as a function of the distance between them showing an oscillating dependence.
- The spectrum for different occupation numbers is studied for different values of Hubbard parameter, the applied electric field and the inter-impurity distance.
- For half-filling ionic to covalent ground state transition are obtained for specific electric field strength.
- Corrections to the mean field approximation are given in order to compute correctly the formation of local magnetic moments in silicene.

Credit author statement

Julián Villarreal and Julián Juan, Paula Jasen and Juan Sebastián Ardenghi: Visualization, Investigation, Reviewing and, Writing- Original draft preparation, Writing- Original draft preparation.

Declaration of interests

☒The authors declare that they have no known competing financial interests or personal relationships that could have appeared to influence the work reported in this paper.

☐The authors declare the following financial interests/personal relationships which may be considered as potential competing interests: